ATM and Artemis promote homologous recombination of radiation-induced DNA double strand breaks in G2

Andrea Beucher, Julie Birraux, Leopoldine Tchouandong, Olivia Barton, Atsushi Shibata, Sandro Conrad, Aaron A. Goodarzi, Andrea Krempler, Penny A. Jeggo, and Markus Löbrich,

Supplementary Materials and methods

Immunofluorescence

For γH2AX and BrdU double staining (Figure 7B), cells were incubated with monoclonal α-γH2AX antibody (Upstate, 1:200) for 1 h and washed in PBS/1% FCS for 3x10 min. Antibodies were cross-linked with PBS/2.5% formaldehyde for 20 min. After three washing steps in PBS/1% FCS, cells were incubated for 1 h at 37°C with α-BrdU-antibody under conditions which generate single-stranded DNA (ssDNA) regions by DNAse treatment (polyclonal sheep, US Biological, 1:200 in 60 mM Tris/HCl, 0,6 mM MgCl2, 1 mM β-Mercaptoethanol, 1 µg/ml DNAse). For the analysis of BrdU resection foci (Figure 5C), double staining with monoclonal α-BrdU antibody (1:200; Becton Dickinson) and polyclonal α-γH2AX antibody (1:200; Upstate) without DNAse treatment was performed. Automated microscopy software (Metasystems, Altlussheim, Germany) was used to generate 2-dimensional plots of γH2AX versus DAPI. G1 and G2 cells were negative for γH2AX whilst S phase cells stained positive due to the presence of aphidicolin, allowing easy and fast discrimination of G1, S and G2 cells using this procedure.

For RPA staining (Figure 5A), cells were extracted for 30 s with cold PBS/0.2% Triton X-100 and fixed with 3% PFA/2% sucrose for 10 min. Cells were washed three times in PBS and incubated with a mixture of primary antibodies (α-RPA, 1:100, Calbiochem and rabbit α-CENP-F, 1:400, Santa Cruz) for 30 min at 37°C. After a series of three washing steps in PBS, samples were incubated with a mixture of goat α-mouse-FITC and sheep α-rabbit-Cy3

(1:200, Sigma Aldrich) for 30 min at 37°C. Cells were washed in PBS three times, incubated with DAPI for 15 min at room temperature, washed with PBS and mounted as described above. For Rad51 staining (Figure 5A), cells were extracted and fixed as described above for RPA, and samples were sequentially stained with rabbit α-Rad51 (1:100, Santa Cruz), donkey α-rabbit-Al488 (1/500, Invitrogen), rabbit α-CENP-F (1:400; Santa Cruz) and sheep α-rabbit-Cy3 (1:200, Sigma Aldrich), each for 30 min at 37°C.

Immunoblotting

To determine the efficiency of siRNA knockdown, HeLa cells were sonicated in lysis buffer (50 mM Tris/HCl pH 8, 150 mM NaCl, 0.5% Natriumdesoxycholat, 1% TritonX100, 0.1% SDS and 1 x complete protease inhibitor cocktail) three times for 1 min and incubated for 30 min at 4˚C. Cell extracts were clarified by centrifugation for 30 min at 13,000 rpm. 1BRneo cells were lysed in lysis buffer (50 mM Tris pH 7.5, 150 mM NaCl, 2 mM EDTA, 2 mM EGTA, 50 mM NaF, 30 mM β-glycerophosphate, 5 mM NaVO4, 0.2 % Triton X-100, 10% NP-40 and 1 x complete protease inhibitor cocktail) for 30 min at 4˚C. Cell extracts were clarified by centrifugation for 10 min at 13,000 rpm. Cell lysates were boiled in SDS loading buffer and 40–100 µg protein was separated using SDS-PAGE. Proteins were transfered to PVDF membrane and immunoblotting was carried out with primary antibody overnight at 4˚C, followed by secondary antibody for 1 h at room temperature. The immunoblots were developed using the ECL reagent (Lumi-Light Western Blotting Substrate, Roche Applied Science). The antibodies used are: α-Brca2 (Cell Signaling Technology, Beverly, MA, USA, #9012, 1:1000), α-Rad51 (Calbiochem, San Diego, CA, USA, PC130, 1:2000), α-Artemis (Novus Biologicals, Littleton, CO, USA, NB 100-542, 1:3000), α-ATM (Abcam, Cambridge, UK, ab31842, 1:500), α-Ku80 (Cell Signaling Technology, Beverly, MA, USA, #2180, 1:1000), α-Lig4 (Acris, Herford, Germany, SP1275, 1:1000), α-GAPDH and α-αTubulin (Santa Cruz, Santa Cruz, CA, USA, 1:1000).

HR reporter assay

To determine the chromosomal HR frequency, NF-DRGP cells (SV40-transformed human skin fibroblasts) stably transfected with a single copy of the pDR-GFP construct were used (a generous gift from Simon Powell). They were grown in DMEM supplemented with 10% FCS, 20 mM Hepes, penicillin (100 I.U./ml), streptomycin (100 μg /ml) and puromycin (2.5 μg /ml). Cells were transfected twice with 0.25 μM siRNA smart pool oligonucleotides (Dharmacon, for Brca2 and ATR knock-down or scrambled RNA; Qiagen, for Artemis knock-down) using Hiperfect transfection reagent (Qiagen). 24 h after the second siRNA transfection, cycling cells were transfected with pEGFP (transfection efficiency control) or pCMV3xnlsI-SceI (functional endonuclease) or phCMV-1 (negative control) using Genejuice reagent (Novagen). Transient expression of I-SceI endonuclease generates a DSB at the integrated GFP gene sequence and stimulates HR. GFP signal was assayed at 3 days post transfection by FACs. For each experiment, 100 000 cells were scored per treatment group and the frequency of recombination events was calculated from the number of GFP-positive cells divided by the transfection efficiency rate for each siRNA type. These values were then normalised so that cells transfected with scrambled RNA (CONT) + pIsceI vector showed 100% inducible GFP value.

Supplementary text to the legend of figure 8

The impact of D37N expression in HSF1 cells leads to a γH2AX repair defect that is slightly greater than loss of Artemis, a feature also observed by expressing D37N in the Artemis null cells. Thus, over-expressed D37N appears to have an effect which is slightly greater than simply inhibition of Artemis activity. Therefore, the slightly greater repair defect is potentially due to an additional impact of the endonuclease inactive D37N mutation on lesions not

otherwise repaired by HR as a consequence of high over-expression. This does not negate the fact that the D37N mutation is unable to complement Artemis null cells and that its over-expression prevents resection in control cells strongly suggesting that the endonuclease activity is required for Artemis function and efficient resection.

Supplementary Figures

Supplementary Figure 1

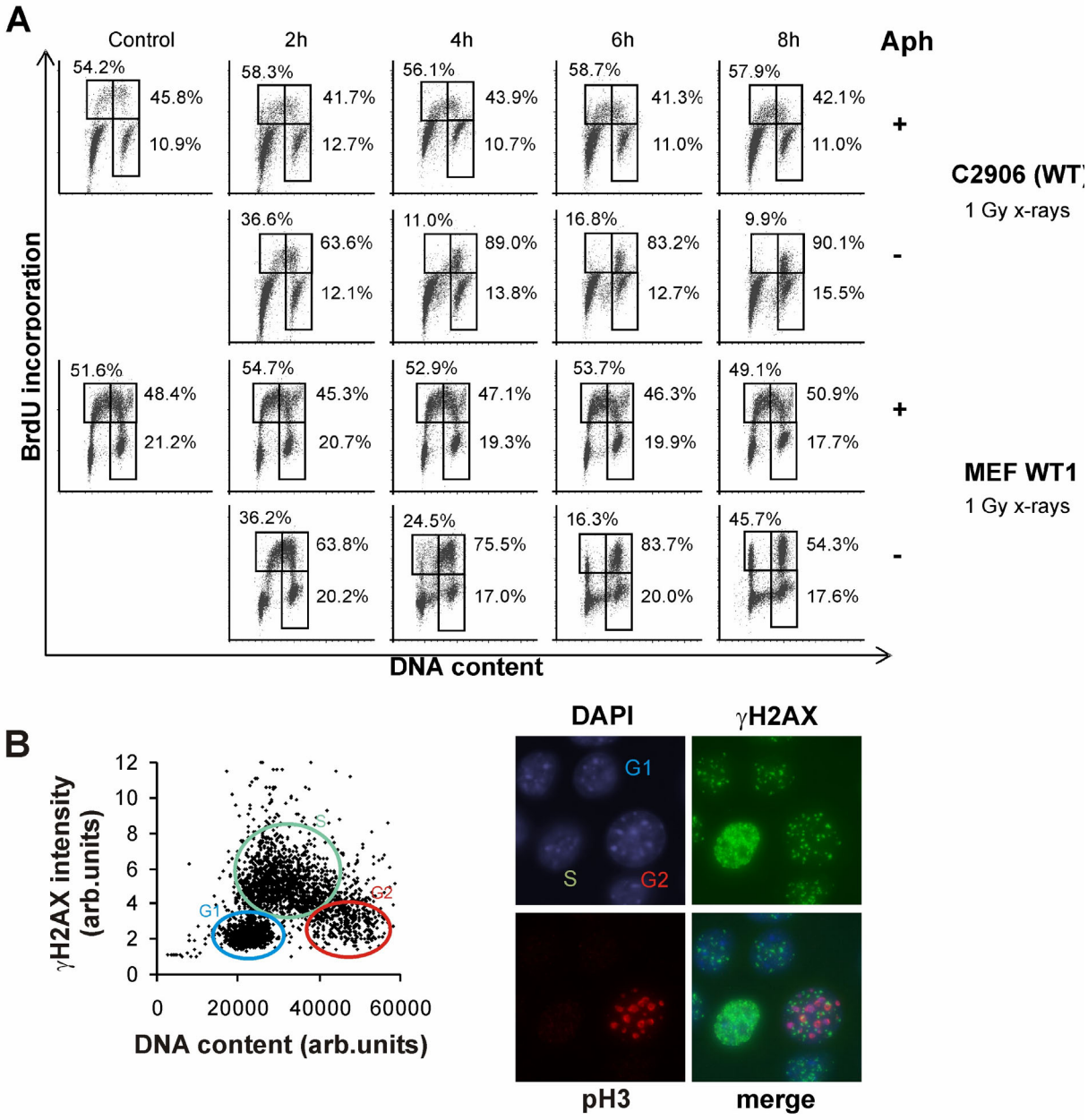

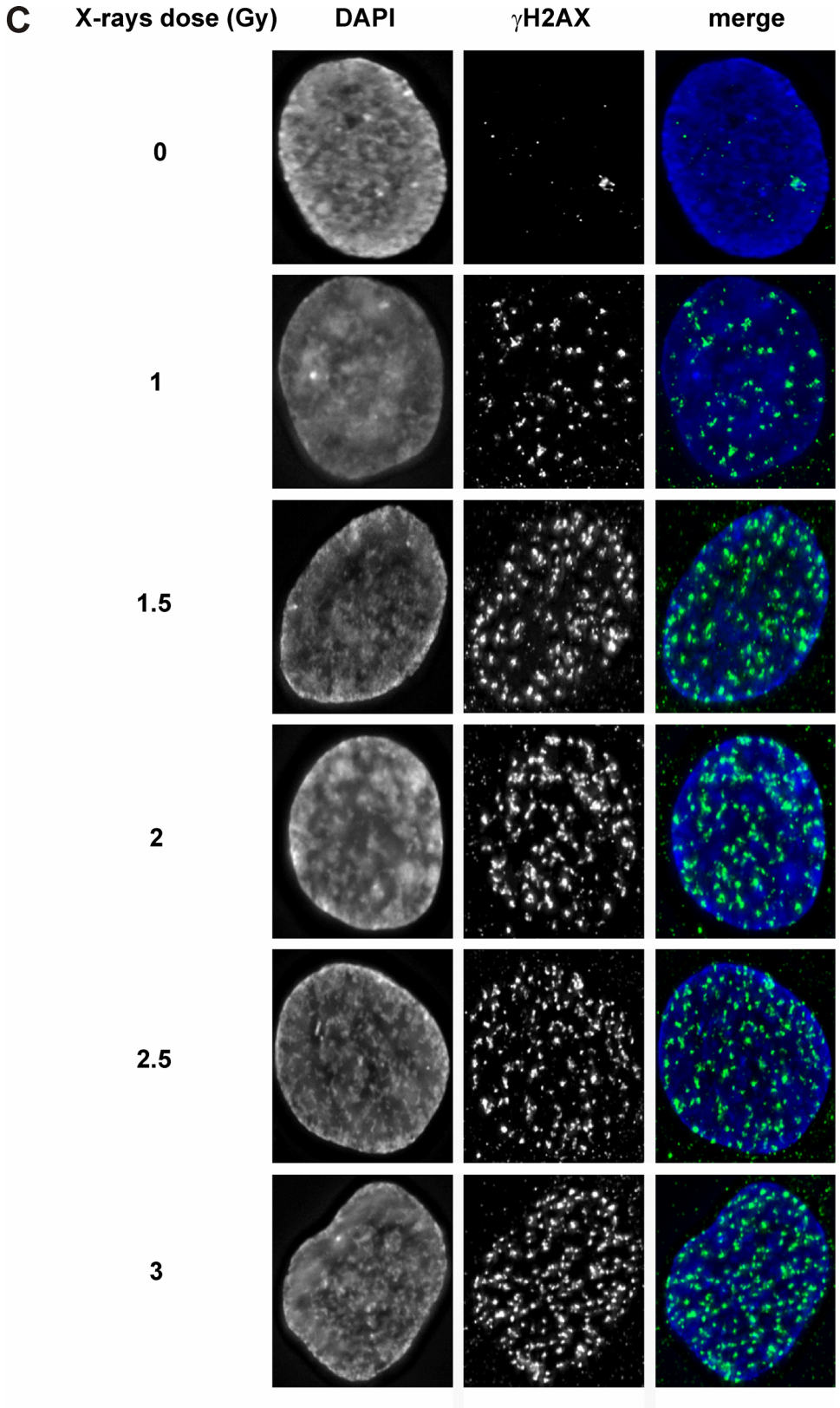
C
X-rays dose (Gy)
DAPI
γH2AX
merge
0
1
1.5
2
2.5
3

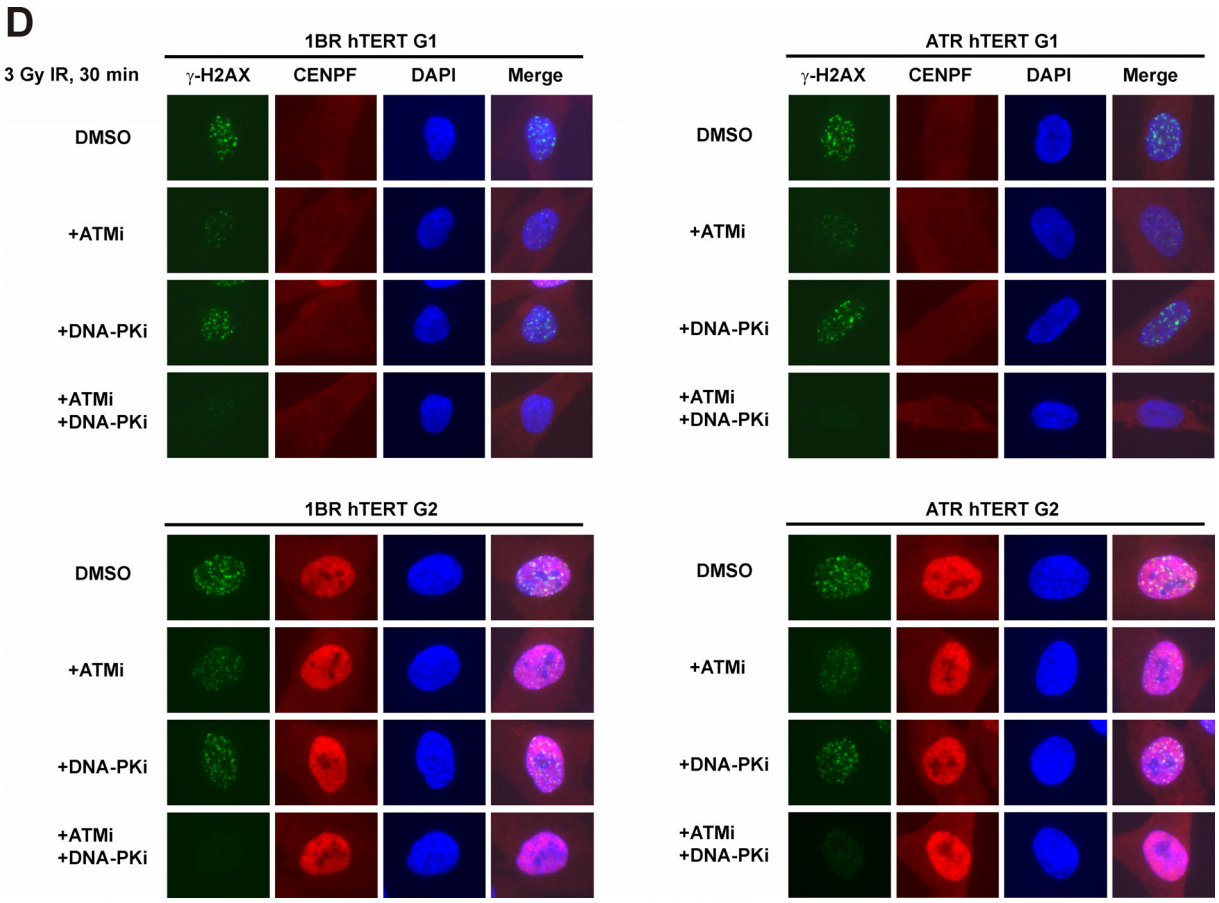
D
3 Gy IR, 30 min
1BR hTERT G1
γ-H2AX
CENPF
DAPI
Merge
DMSO
+ATMi
+DNA-PKi
+ATMi
+DNA-PKi
ATR hTERT G1
γ-H2AX
CENPF
DAPI
Merge
DMSO
+ATMi
+DNA-PKi
+ATMi
+DNA-PKi
1BR hTERT G2
DMSO
+ATMi
+DNA-PKi
+ATMi
+DNA-PKi
ATR hTERT G2
DMSO
+ATMi
+DNA-PKi
+ATMi
+DNA-PKi

Supplementary Figure 1: (A) Representative FACs plots of primary human fibroblasts and MEFs in the presence or absence of aphidicolin. Cells were BrdU labeled for 1 h, irradiated with 1 Gy immediately after labeling, and aphidicolin was added. The top rectangles show the percentages of BrdU-positive cells in early versus late S phase. The bottom rectangle indicates the percentage of BrdU-negative cells in G2. **(B)** Identification of cell cycle phases in MEFs using phosphoH3 (pH3) instead of CENP-F as a marker for G2. Cells were scanned under the microscope and the γH2AX signal was plotted against the DAPI signal. Cells with an intermediate DAPI signal, no pH3 signal and a high pan-nuclear γH2AX signal represent S phase cells with stalled replication forks due to the aphidicolin treatment. G2 phase cells were identified by broad focal pH3 staining, high DAPI signal and a dotted instead of a pan-nuclear γH2AX signal. G1 cells were low in DAPI content, and negative for pH3 and the high pan-nuclear level of γH2AX phosphorylation. Although G2 and M phase cells both stain positively for pH3 they are readily distinguished by the specific pattern of broad focal staining of G2 cells whereas M phase cells show a pronounced pan-nuclear pH3 signal (Hendzel et al., 1997, Mitosis-specific phosphorylation of histone H3 initiates primarily within pericentromeric heterochromatin during G2 and spreads in an ordered fashion coincident with mitotic chromosome condensation. *Chromosoma.* 106:348-360). Mitotic cells are also readily distinguished by condensed chromatin. **(C)** Representative high-resolution images of γH2AX foci formation in G2 phase HSF1 cells analysed at 15 min after IR. Images were taken using an epifluorescent Axiovert 200M microscope with a 100x Plan-Neofluar objective using Axiovision software (Zeiss, Jena, Germany) (number of z-slices = 15; distance between z-slices = 275 nm). Z-slices were deconvolved using the Maximum Likelihood Estimation function and superimposed using the Maximum Intensity Projection function of Huygens software (SVI Hilversum, The Netherlands). No adjustment for background staining or contrast enhancement was undertaken. **(D)** Induction of γH2AX phosphorylation after IR in G1 and G2 is dependent on ATM and DNA-PKcs. WT and ATR deficient human fibroblasts show an identical γH2AX signal suggesting that ATR does not significantly contribute to

γH2AX foci formation after IR. Moreover, cells treated with the ATM inhibitor KU55933 (designated ATMi in the figure) and the DNA-PK inhibitor NU7026 (designated DNA-PKi) do not show γH2AX foci following IR.

Supplementary Figure 2

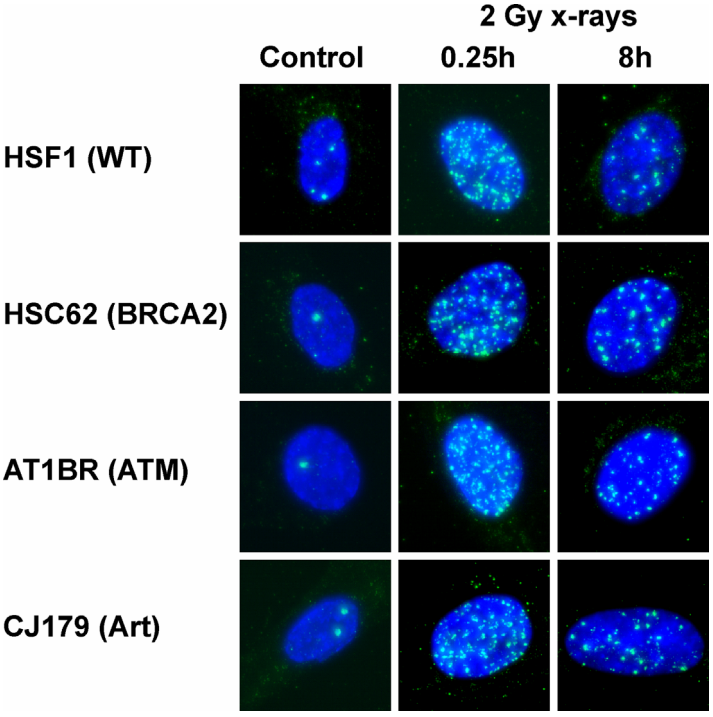

Supplementary Figure 2: Representative images of spontaneous and IR-induced γH2AX foci formation in G2 phase primary human fibroblasts. Cells deficient for Brca2, Artemis or ATM show a similar level of initial γH2AX foci but elevated unrepaired foci numbers compared to WT cells.

Supplementary Figure 3

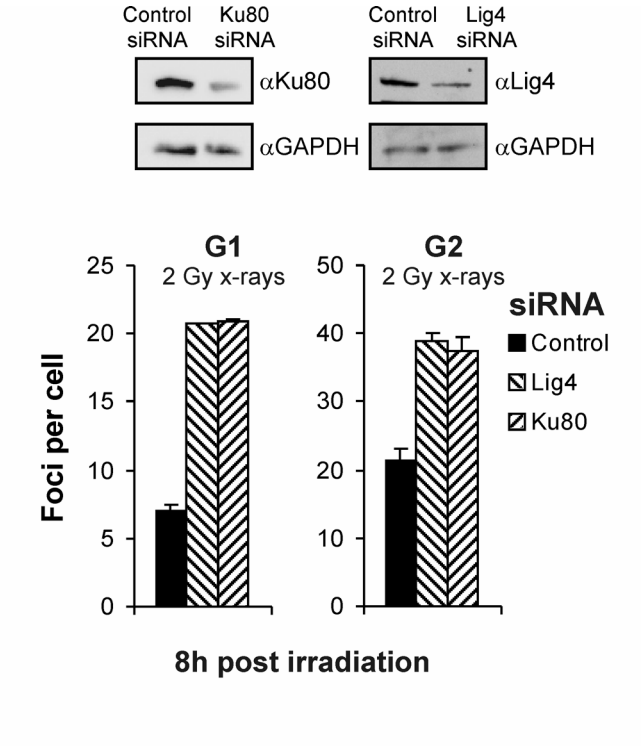

Supplementary Figure 3: Control experiments showing the efficient down-regulation of Ku80 and DNA ligase IV in siRNA treated HeLa cells by Western blotting and γH2AX foci analysis at 8 h after 2 Gy.

Supplementary Figure 4

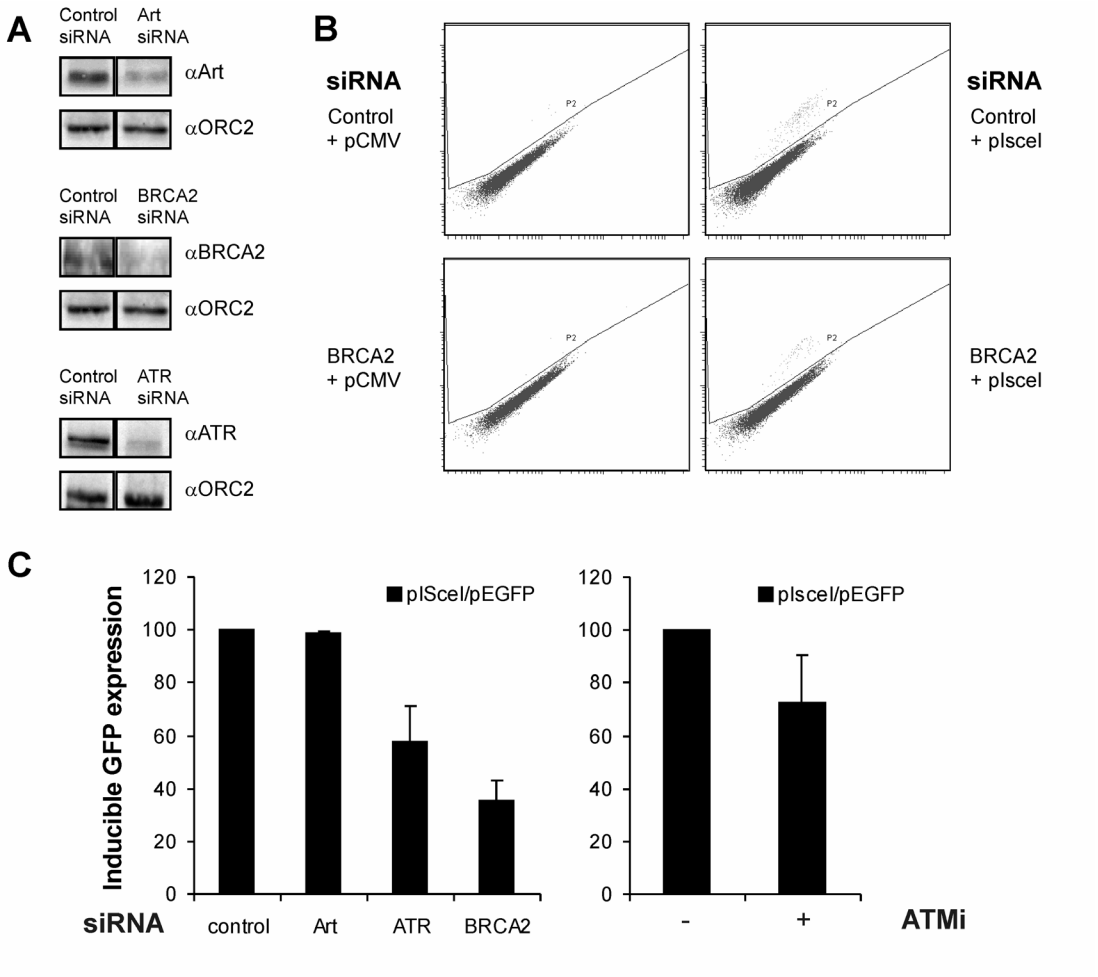

Supplementary Figure 4: I-SceI induced HR does not require Artemis. **(A)** Immunoblots showing the efficiency of siRNA knock-down in DRGP cells (SV40-transformed human fibroblasts) analysed 72 h after transfection. **(B)** Representative FACs analyses of DRGP cells treated with control or Brca2 siRNA. HR was measured by dual-color FACs detection of GFP positive cells. Left panels show cells without DSB induction, exhibiting few GFP positive

cells. Right panels show cells 3 days after transfection with I-SceI expression plasmid. pGFP plasmid transfection was performed to measure the percentage of cells expressing transiently expressed plasmid (not shown). HR frequency (%) was calculated as the proportion of GFP positive cells after I-SceI transfection, divided by the proportion of GFP positive cells after pGFP transfection. **(C)** HR frequencies for DRGP cells treated with control, Artemis, ATR, or Brca2 siRNA (left panel) or treated with the ATM inhibitor KU55933 (designated ATMi in the figure) (right panel). Chemical inhibition of ATM was found to be more robust and therefore used instead of ATM siRNA treatment. Error bars represent the SEM from the analysis of at least 3 different experiments.

Supplementary Figure 5

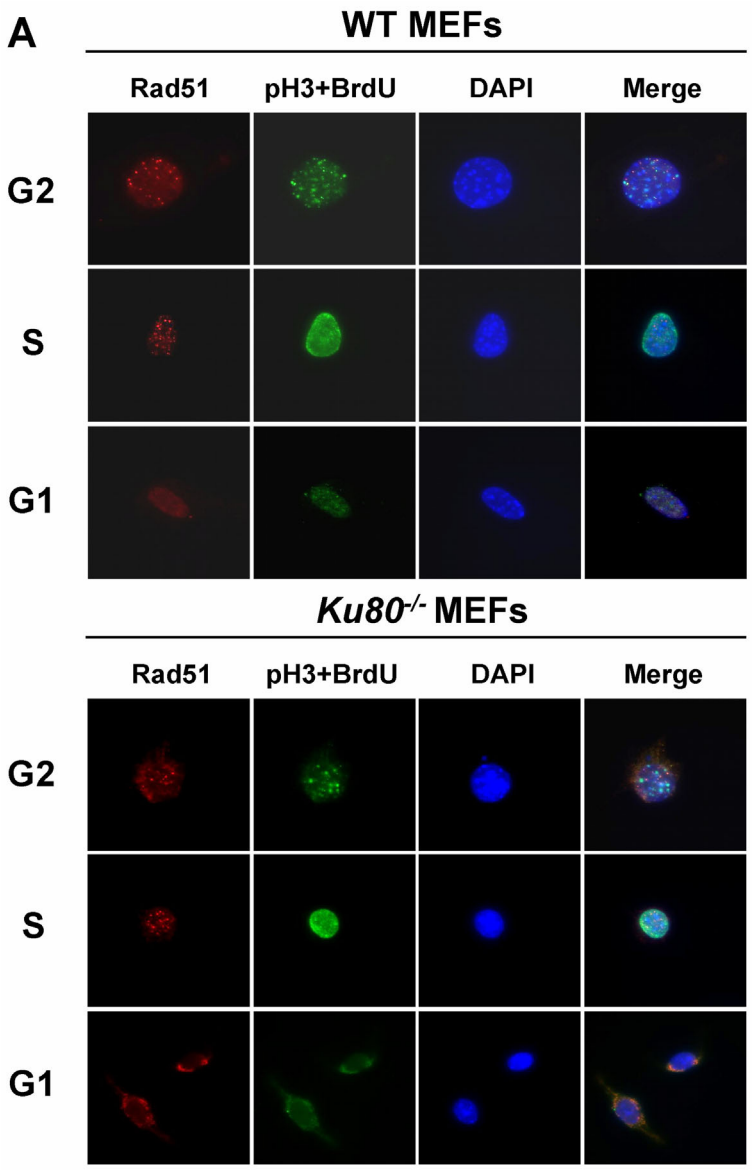

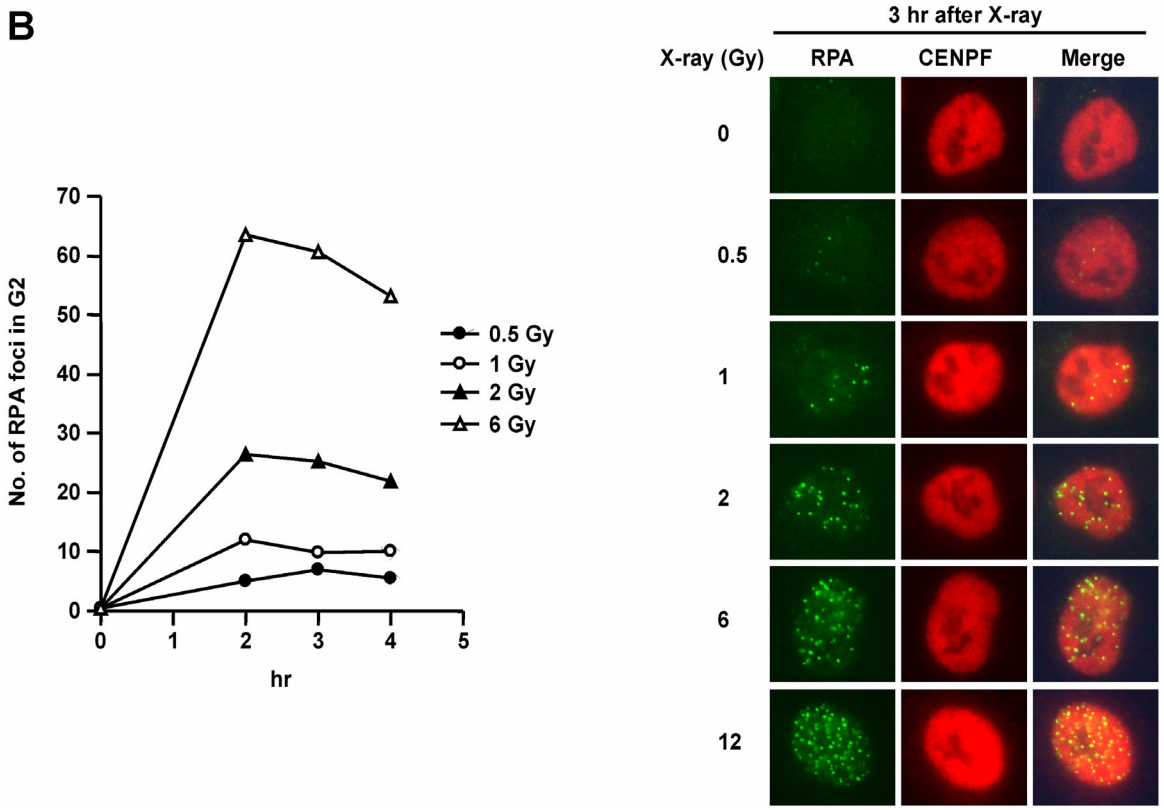
B
No. of RPA foci in G2
hr
0.5 Gy
1 Gy
2 Gy
6 Gy
3 hr after X-ray
X-ray (Gy)
RPA
CENPF
Merge
0
0.5
1
2
6
12

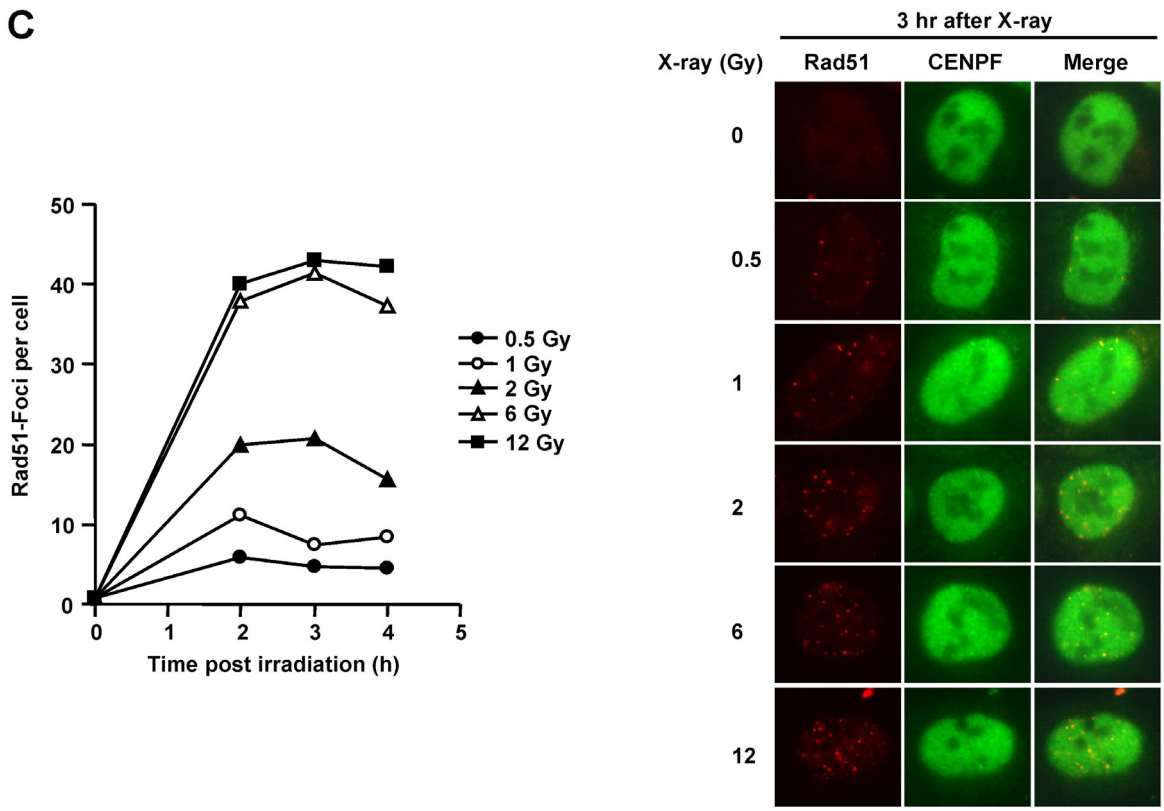
C
Rad51-Foci per cell
Time post irradiation (h)
0.5 Gy
1 Gy
2 Gy
6 Gy
12 Gy
3 hr after X-ray
X-ray (Gy)
Rad51
CENPF
Merge
0
0.5
1
2
6
12

Supplementary Figure 5: (A) Rad51 foci form only in S and G2 phase but not in G1 phase of WT or Ku80$^{-/-}$ MEFs. **(B)** Kinetics for RPA foci formation after various X-ray doses. Foci formation is approximately linear up to 60 foci per cell obtained at a dose of 6 Gy. After 12 Gy X-rays, about 100 foci per cell are formed but quantification becomes uncertain in this range. **(C)** Kinetics for Rad51 foci formation after various X-ray doses. Rad51 foci reach a saturation value at about 40 foci; up to this level foci formation is approximately linear.

Supplementary Figure 6

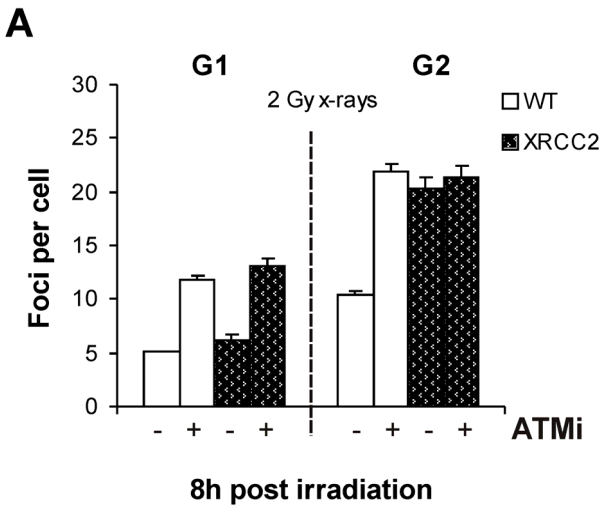

Supplementary Figure 6: (A) γH2AX foci analysis in XRCC2$^{-/-}$ MEFs in the presence or absence of the ATM inhibitor KU55933 (designated ATMi in the figure). The analysis was carried out as for Figure 2B.

Supplementary Figure 7

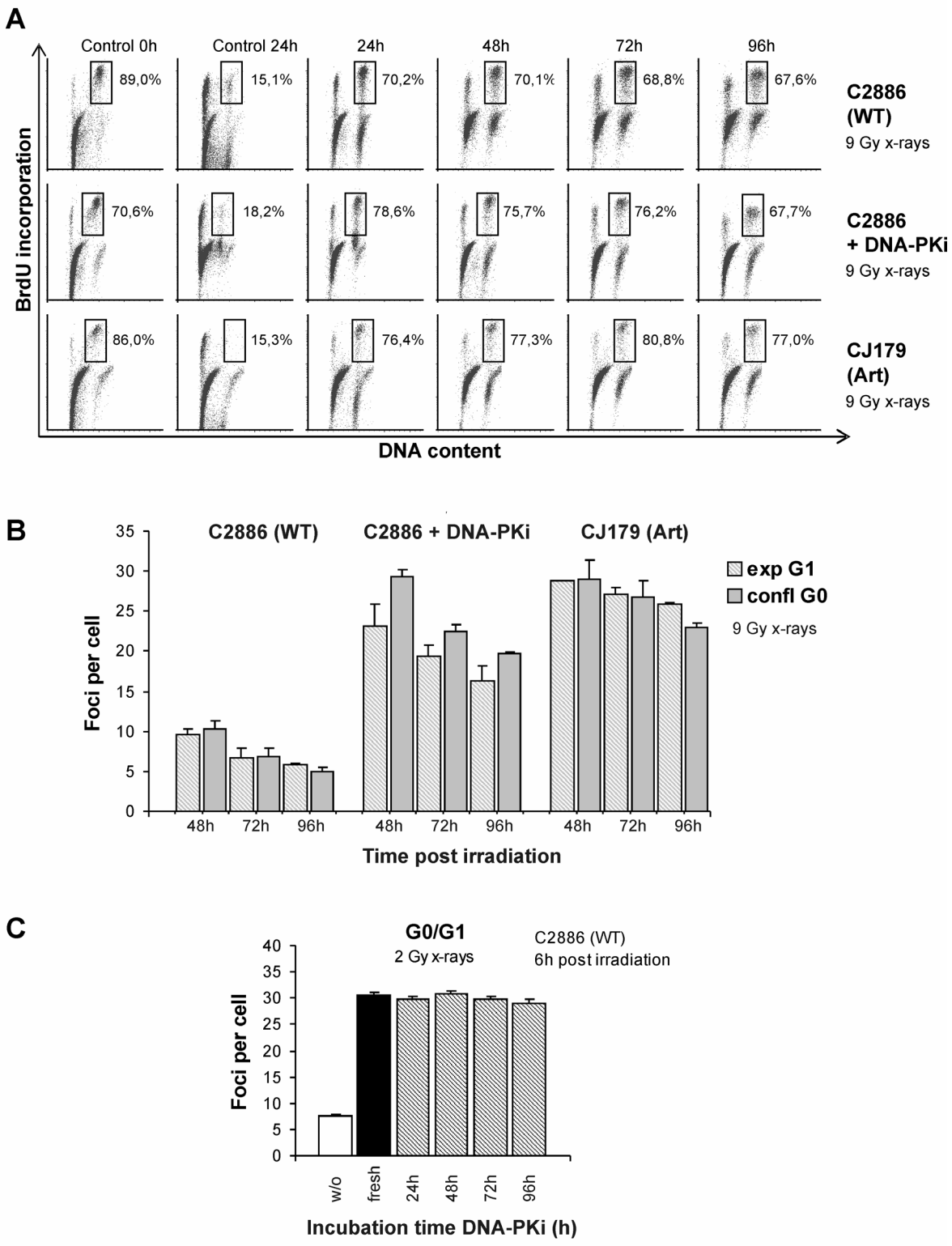

Supplementary Figure 7: (A) Representative FACs plots showing the percentage of BrdU-labeled primary human fibroblasts in G2 at 0, 24, 48, 72 and 96 h after 9 Gy X-irradiation (rectangles). Irradiation was performed 4 h after BrdU labeling. **(B)** DSB levels in confluent G0 versus growing G1 cells. G1 cells were obtained from the analysis of BrdU negative cells in the same samples that were analysed for the G2 data in Figure 7B. The G0 and G1 values are identical for WT and Artemis deficient cells. For WT cells treated with the DNA-PK inhibitor NU7026 (designated DNA-PKi), G1 values are slightly lower than G0 values possibly reflecting the fact that the BrdU negative cell population contains a small but significant proportion of G2 phase cells (see panel A) which shows DSB rejoining in the absence of DNA-PKcs. **(C)** Control experiment for Figure 7B demonstrating the continuing activity of NU7026 over 4 days. Medium with NU7026 was used immediately after preparation or was incubated on cell cultures for up to 96 h and than tested for its ability to inhibit DSB repair. The elevation in the level of γH2AX foci was identical for all samples showing that the activity of NU7026 remains unaffected over a 4-day incubation period.

Supplementary Figure 8

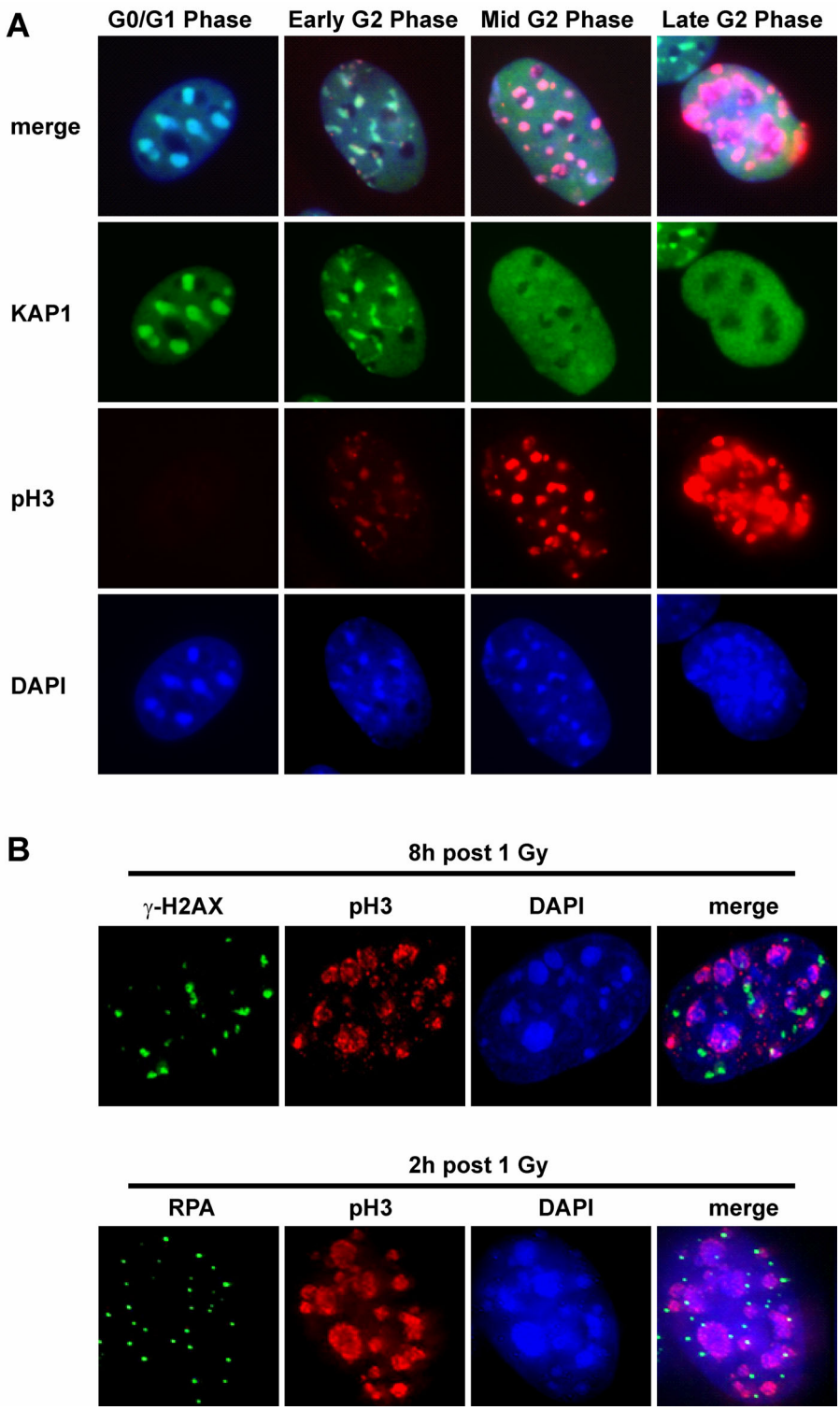

Supplementary Figure 8: (A) Representative images of KAP-1 and DAPI signal of G0/G1, early G2, middle G2 and late G2 phase NIH 3T3 mouse cells modified from Goodarzi *et al* (2009). pH3 signal intensity allowed the discrimination of early, middle and late G2 cells. **(B)** Localization of γH2AX foci (assessed at 8 h post 2 Gy in NIH 3T3 mouse cells treated with the ATM inhibitor KU55933) and RPA foci (assessed at 2 h post 2 Gy in untreated NIH 3T3 cells) in middle G2 phase cells, identified by pH3 staining. The random γH2AX and RPA foci distribution correlates with the random KAP-1 distribution in middle G2 cells (see panel A).